JMEPEG (2011) 20:463–467
DOI: 10.1007/s11665-010-9705-2

1059-9495/$19.00

TEM Analysis on Micro-Arc Oxide Coating on the Surface of Magnesium Alloy

Yuan-Sheng Huang and Hong-Wei Liu

(Submitted January 21, 2009; in revised form May 31, 2010)

By micro-arc oxidation (MAO), the oxide coatings were prepared on the surface of magnesium alloys in a composite electrolytic solution. The microstructures of the coating layer and the interface between coating and substrate were analyzed by using transmission electron microscopy (TEM) and scanning electron microscopy (SEM). The oxide coating consists of two layers (the outer and the inner layer). Although both layers are composed of microcrystalline MgO and amorphous phase, the inner layer is more compact and rich in fluorine with a thickness of about 1-2 μm. Fluorine plays an important role in the inner dense layer formation. The inner layer, like a barrier wall, blocks the thickness of the oxide coating to increase and improves corrosion resistance. The formation mechanism of the inner layer is also discussed.

Keywords interface, magnesium alloy, micro-arc oxidation, transmission electron microscopy (TEM)

1. Introduction

Micro-arc oxidation (MAO) is an energy-consumption process, always accompanied by plasma chemical, electrochemical, and physics chemical reactions in the micro-arc discharge channels (Ref 1). Therefore, the formation process of the oxide coating was very complex. By far, there is not a universal model that can roundly interpret the oxide coating formation. The influencing factors include many technic parameters such as voltage, current density, frequency, temperature, and conductance of electrolyte. The corrosion resistance, microstructure, and elemental composition would be changed with the electrolyte compositions. After being treated by the micro-arc oxidation (MAO), magnesium alloy had a good anti-corrosion and a good hardness because of the micro-arc oxide coating formation on it. MgO is a universal phase forming in all kinds of electrolyte. In general, $MgSiO_3$, $MgA1_2O_4$, and $Mg_3(PO_4)_2$ form in sodium silicate, sodium aluminate, and phosphate systems, respectively (Ref 2-5). The complex phases such as $Mg_3Al_2Si_3O_{12}$, $(Mg_4Si_2)O_{20}$, and δ-$MgAl_{28}O_{40}$ have also been reported (Ref 6).

The oxide-coating formation includes two stages (Ref 7, 8). The increase of coating-thickness depended, at the first stage, on the coating surface advancing toward the outside, and, at the second stage, on the coating/substrate interface toward the substrate. Previous researchers (Ref 1-3) argued that the oxide coating included two layers: the outer loose layer with many micro-holes, and the inner dense layer. There was a transition layer being composed of Mg and intermetallic compound between the inner dense layer and the substrate. However, the study on the coating/substrate interface and the microstructure of the inner dense layer is seldom reported. In this article, the coating/substrate interface was analyzed using TEM and SEM. A thin inner layer adjacent to the substrate was found in the oxide coating. The formation mechanism of the inner layers was discussed.

Yuan-Sheng Huang, Department of Materials Technology, Jiangmen Polytechnic, Jiangmen 529000, Guangdong, People's Republic of China and **Hong-Wei Liu**, College of Materials Science and Engineering, Guangxi University, Nanning 530004, People's Republic of China. Contact e-mails: hwliu@gxu.edu.cn and nightofgz@163.com.

2. Experimental Details

The elemental composition of magnesium alloy used in this study was 90.21% Mg + 8.56% Al + 0.41% Zn + 0.82% Mn (wt.%). The specimen size was 50 × 30 × 5 mm. MAO equipment was self-made with a type of MOP-60 IGBT. The threshold power was 42 kW. The electrolyte composition and technological conditions were shown in Table 1. The dissolvent was distilled water. The technological process route was as follows: sample preparing → polishing → cleanout → degreasing → micro-arc oxidation → examination.

For transformation electron micrograph (TEM) observation, XTEM samples of 3 mm in diameter were prepared for subsequent ion-thinning. The TEM samples were examined using a Philips Tecnai F20 transmission electron microscope equipped with an energy-dispersive x-ray analysis system. The cross-sectional morphology was examined using SEM with a LEO 1530 VP.

3. Results and Discussion

3.1 Microstructure

Figure 1 shows the TEM morphology of the micro-arc oxide coating and magnesium alloy substrate. TEM observation reveals that the oxide coating includes two layers, namely the outer layer and the inner layer as shown in the TEM bright field (BF) image (Fig. 1a). Figure 1(c) and (d) are the diffraction patterns of magnesium substrate down [0001] and $[2\bar{1}\bar{1}0]$ taken

from variant selected areas. In order to distinguish the inner layer, dark field (DF) technology is employed. Figure 1(b) is the DF image corresponding to Fig. 1(a) taken by using the substrate diffraction spot $(01\bar{1}0)$. The inner layer appears like a dark strip along the coating/substrate interface. Figure 1(e) and (f) show the diffraction patterns of the outer layer and the inner layer, respectively. It is clear that both of them are composed of multicrystalline magnesia and a bit of amorphous phase. Figure 2 gives the long-range DF morphology of the inner layer. The thickness of the inner layer is about 1-2 μm. In Fig. 3 is shown an SEM image, in which the inner layer is marked. Table 2 provides the thickness values of the inner layers collected from seven measuring points. It reveals that the thickness of the inner layer is not more than 1.5 μm. In-set of Fig. 3 indicates that there is no observed defeat in the inner layer. As a comparison, there are many defects such as holes in the outer layer. From TEM and SEM observation, the inner layer is denser than the outer layer. The inner layer and substrate embed in each other along their interface, and no microhole is found. This is beneficial to improving adhesion. The compact inner layer also enhances the corrosion resistances of magnesium alloy.

Table 1 Electrolyte composition and technological conditions

KOH	Na_3PO_4	Na_3AlF_6	Current density	Temperature	Oxidation time
50 g L^{-1}	40 g L^{-1}	15 g L^{-1}	20 A dm^{-2}	20-40 °C	30 min

3.2 EDX Analysis

The elemental compositions of the outer layer, inner layer, and substrate were determined by energy dispersion spectroscopy (EDS). Figures 4 and 5 give the result. From Fig. 4, the magnesium-alloy substrate is mostly composed of magnesium and aluminium, while the outer layer is mainly composed of magnesium and oxygen. From the line analysis of EDS shown in Fig. 4, oxygen gets evenly distributed over the outer layer (Fig. 5g), whereas the layer exhibits a gradient distribution in the Mg concentration from the surface to the inner part (Fig. 4d). Both aluminum and zinc have very insignificant presence (Fig. 4e, f). Figure 5 shows the barrier element analysis. Apparently, there are magnesium, oxygen, aluminium, zinc, and fluorine in the inner layer, but both aluminium and zinc are found in very small fractional amounts. According to our observation, only the inner layer is rich in fluorine.

3.3 Discussion

Wang et al. (Ref 2) have reported the micro-arc oxide coating inclusive of two layers. One is the outer layer in which there are a lot of micro-holes; the other is an inner dense layer. The inner layer is thicker, with its thickness being about 80% of the coating. The outer layer showed a bad corrosion resistance since the corrosive media can penetrate through the layer along the micro-hole. In general, the oxide coating was composed of magnesium, oxygen, aluminum, silicon, and phosphor. As for fluorine, Wang et al. (Ref 2) reported that there existed a fluoride-enriched zone of about 3-5 μm at the coating/substrate interface as confirmed by SEM observation,

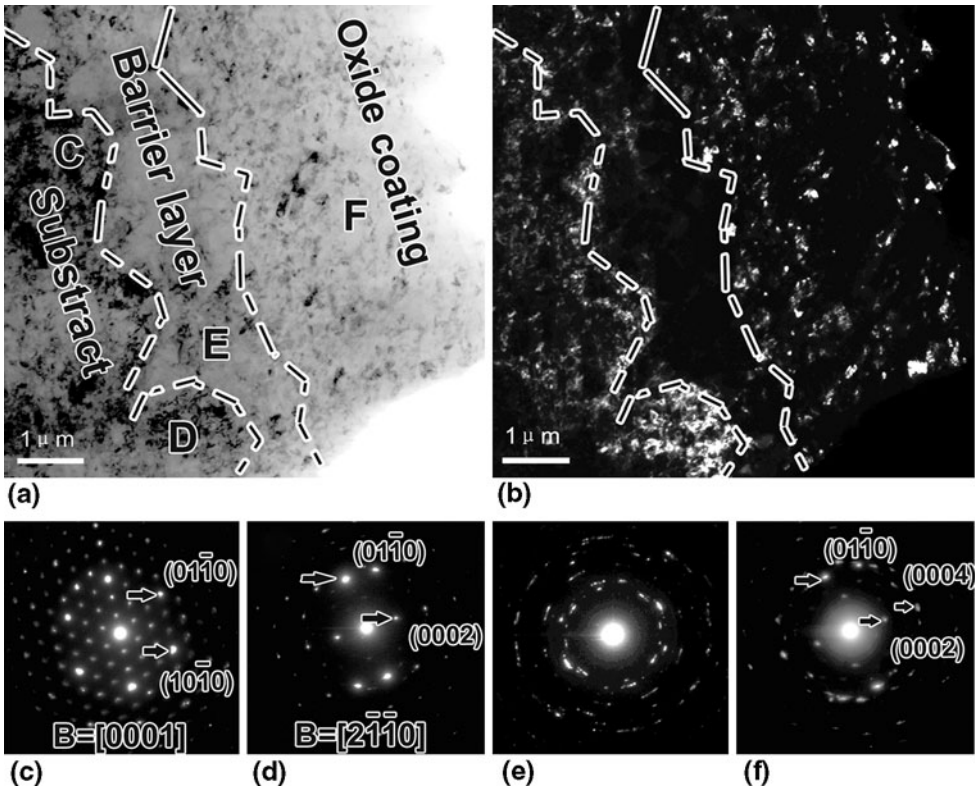

Fig. 1 TEM micrographs of micro-arc coating on the surface of magnesium alloy. (a) Bright field image which shows microstructure of this coating. (b) Corresponding dark field image taking by using diffraction spot $(01\bar{1}0)$. (c, d) Diffraction patterns taken from magnesium substrate and can be indexed as [0001] and $[2\bar{1}\bar{1}0]$, respectively. (e, f) Diffraction rings taken from barrier layer and coating

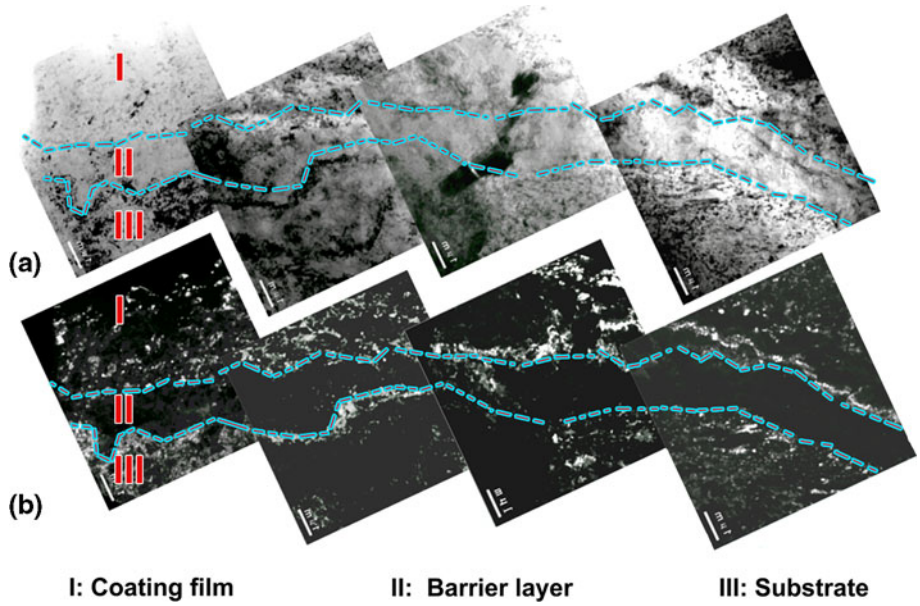

Fig. 2 TEM micrographs showing long-range morphology of the inner layer. (a) Bright field images and (b) is the corresponding dark field images

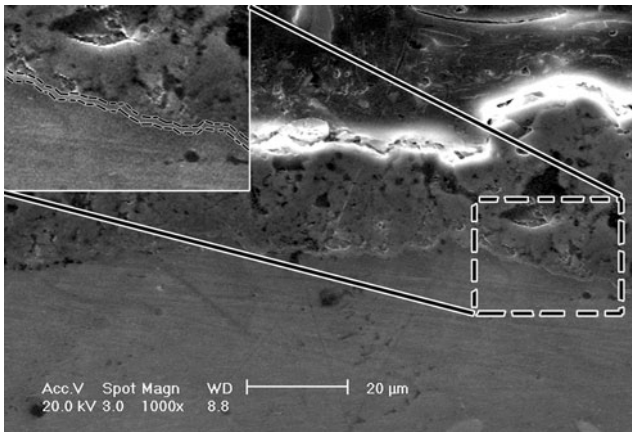

Fig. 3 SEM morphology of the oxide coating, barrier layer, and substrate

Table 2 Thickness of the inner layer

Example number	1	2	3	4	5	6	7
Thickness, µm	0.9	0.9	1.1	1.1	1.3	1.3	1.5

but there was no detailed analysis on the effect of fluoride on the coating. However, the inner layer observed by the authors of this article is not more than 1.5 µm. It is believed that the value as observed in this study is more exact since the TEM analysis can give a clearer interface of two layers. Up to now, the formation mechanism of the oxide coating has not been completely clear yet, especially, as there are few reports on the microstructure of the inner layer and the effect of fluorine on the oxide coating.

During coating by MAO, the micro-arc spark discharge resulted in a high-temperature-zone formation between the oxide coating and the substrate, and the alloy in the zone got melted (Ref 9). The molten alloy reacted with oxygen to form MgO which then became solidified when the micro-arc spark discharge broke off. The coating thickness was determined by the oxygen diffusion toward the substrate when it was reaching a critical value. Oxygen diffused through the inner layer to react with magnesium. Oxygen played a vital role in determining the intensity and size of sparks, and the abundant oxygen resulted in the intensive sparks (Ref 9).

According to the observation of this study, there is an inner compact layer along the interface between the oxide coating and the substrate. Although the diffraction patterns show that both the inner and outer layers are composed of multicrystalline magnesia and a bit of amorphous phase; the dark field observation, the elemental composition, and their density indicate that the inner layer are different from the outer layer. The inner compact layer is beneficial to enhancing the corrosion resistance of magnesium alloy since it is difficult for the erosive media to penetrate through the inner layer to rot the substrate (Ref 5, 10, 11).

In accordance with the formation process of the oxide coating, it is believed oxygen goes through the inner layer and makes the thickness of the oxide coating increase, and the inner dense layer and the fluorine rich in it prevent the oxide coating from continuing to increase in thickness. The inner layer moving toward the substrate depends not only on the MAO technological parameters but also on the element diffusion. Due to the obstruction of the oxide coating with a larger thickness, the spark discharge is faint in intensity. It is very difficult for oxygen to diffuse and reach the interface between the inner layer and the substrate. Fluorine diffusing and accumulating in the inner layer baffles the diffusion of oxygen. Therefore, the inner layer moves very slowly. In order to obtain a compact and stable inner layer, fluorine is a necessary element. Fluoride is very stable and has a good corrosion resistance (Ref 5). Apparently, the formation of the inner layer is related to the faint spark discharge and the oxygen and fluorine accumulation. Thus, the inner layer blocks

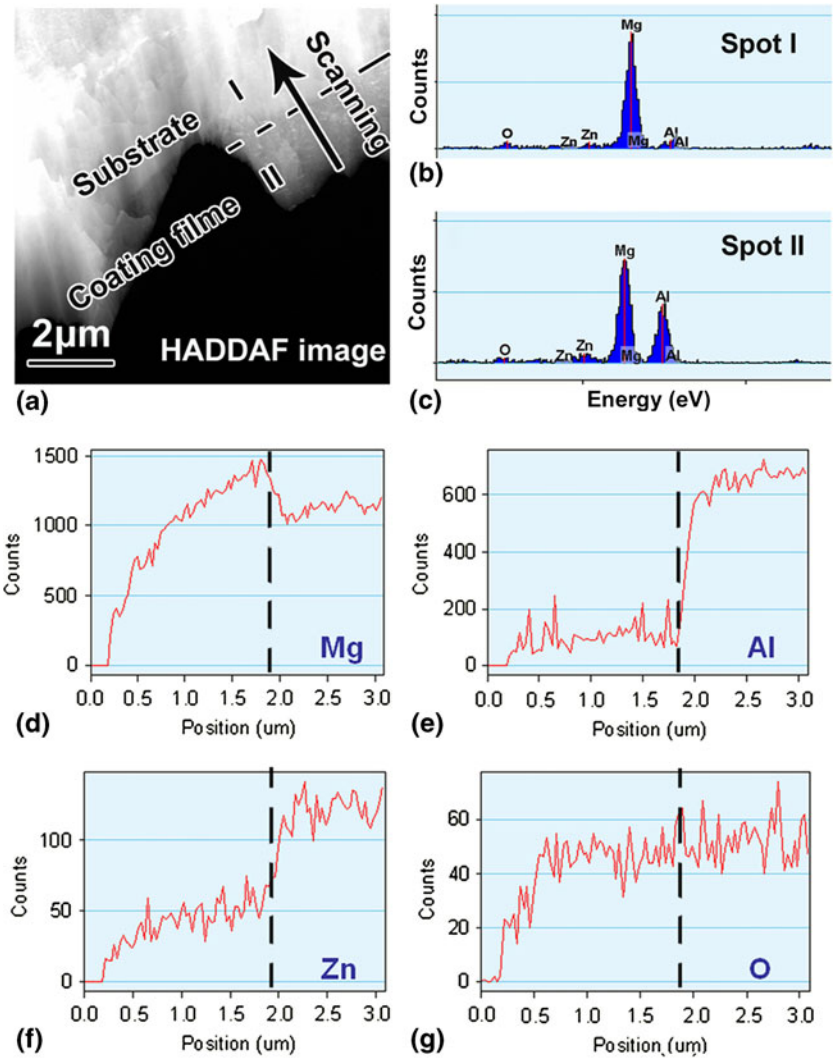

Fig. 4 EDS analysis: (a) HADDAF image of coating film; (b, c) spot profiles of the selected areas (a) and (b), respectively. EDS analysis of position A; (c) EDS analysis of position (b). (d-g) Line profiles corresponding elements Mg, Al, Zn, and O, respectively

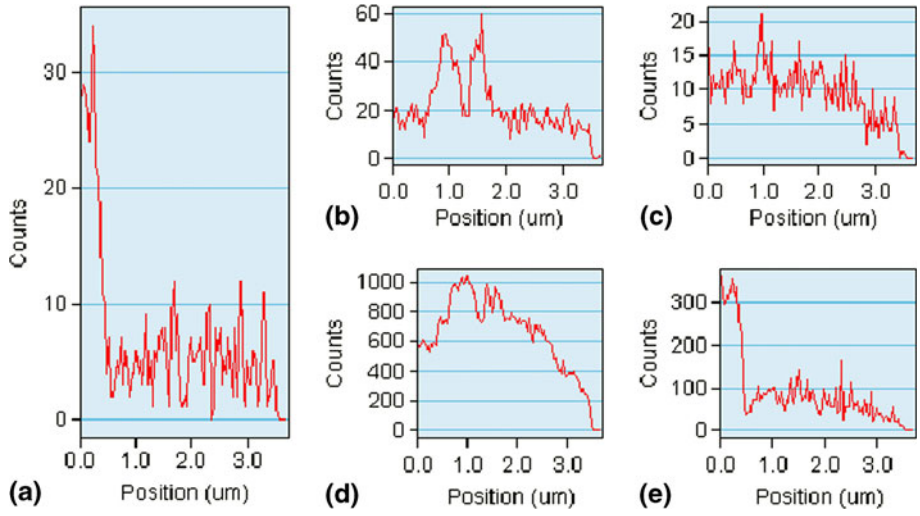

Fig. 5 EDS line analysis of the barrier layer. (a-e) Line profiles of element Zn, O, F, Mg, and Al, respectively

MAO to proceed, and it is difficult for the thickness of the inner layer to grow up to 2 μm.

4. Conclusion

The oxide coating includes two layers (the outer layer and the inner layer). Although both layers are composed of microcrystalline MgO and amorphous phase, the inner layer is more compact and rich in fluorine, about 1-2 μm thickness. Fluorine plays an important role in the inner dense layer formation. The inner layer, like a barrier wall, blocks the thickness of the oxide coating to increase and improves corrosion resistance.

Acknowledgments

This study was financially supported by the Initial Research Fund for Doctoral scholars Sponsored by Guangxi University, China under grant numbers DD010010 and Jiangmen Science and Technology Project, Guangdong Province, China.

References

1. H.F. Guo, M.Z. An, S. Xu, and H.B. Huo, Formation of Oxygen Bubbles and Its Influence on Current Efficiency in Micro-Arc Oxidation Process of AZ91D Magnesium Alloy, *Thin Solid Films*, 2005, **485**, p 53–58
2. L.S. Wang, Q.Z. Cai, B.K. Wei, and Y.W. Yan, Analyses of Microarc Oxidation Coating Formed on AZ91D Alloy in Phosphate Electrolytes, *J. Wuhan Univ. Technol.: Mater. Sci. Ed.*, 2007, **22**, p 229–233
3. H.F. Guo, M.Z. An, H.B. Huo, S. Xua, and L.J. Wu, Microstructure Characteristic of Ceramic Coating Fabricated on Magnesium Alloys by Micro-Arc Oxidation in Alkaline Silicate Solutions, *Appl. Surf. Sci.*, 2006, **252**, p 7911
4. Z.H. Jiang, X.B. Zeng, and Z.P. Yao, Preparation and Structure of Microarc Oxidation Ceramic Coatings Containing ZrO_2 Grown on LY12 Al Alloy, *Rare Met.*, 2006, **25**, p 270
5. H.F. Guo and M.Z. An, Growth of Ceramic Coatings on AZ91D Magnesium Alloys by Micro-Arc Oxidation in Aluminate Fluoride Solutions and Evaluation of Corrosion Resistance, *Appl. Surf. Sci.*, 2005, **246**, p 229
6. Z.L. Wei, Q.R. Chen, and X.C. Guo, Microstructure and Corrosion Resistance of Ceramic Coating on Magnesium Alloys, *Mater. Prot.*, 2003, **36**, p 21
7. J.M. Albella, I. Montern, and D.J.M. Martine, Electron Injection and Avalenche During the Anodic Oxidation of Tatanium, *J. Electrochem. Sci*., 1984, **131**, p 1101–1104
8. W. Krysmann, P. Kurze, K.H. Dittrich, and H.G. Schneider, Process Characteristics and Parameters of Anodic Oxidation by Spark Discharge (ANOF), *Cryst. Res. Technol.*, 1984, **19**, p 973–979
9. Y.H. Wang, J. Wang, J.B. Zhang, and Z. Zhang, Effects of Spark Discharge on the Anodic Coatings on Magnesium Alloy, *Mater. Lett.*, 2006, **60**, p 474–478
10. A. Bai and Z.J. Chen, Effect of Electrolyte Additives on Anti-corrosion Ability of Micro-Arc Oxide Coatings Formed on Magnesium Alloy AZ91D, *Surf. Coat. Technol.*, 2009, **203**, p 1956–1963
11. L.C. Zhao, C.X. Cui, Q.Z. Wang, and S.J. Bu, Growth Characteristics and Corrosion Resistance of Micro-Arc Oxidation Coating on Pure Magnesium for Biomedical Applications, *Corrosion Sci*., 2010, **52**, p 2228–2234